Coupled 3D Numerical Simulations of the Effects of Ocean Salinity on Tropical Cyclone Intensity

James A. Hlywiak* and David S. Nolan

University of Miami, Miami, FL

1 Introduction

In many modeling studies focusing on air-sea interactions in tropical cyclones (hereafter TCs), upper ocean stability is approximated by the vertical temperature profile, and gradients in salinity are assumed to be negligible. However, in certain instances freshwater inputs at the surface create a shallow, low salinity mixed layer above strong gradients in salinity at the base of the layer. When this occurs, the upper ocean becomes more stratified, thus increasing the ocean's resistance to entrainment mixing of cooler, sub-thermocline waters into the surface mixed layer due to a given wind stress from a passing TC. This phenomenon was first observed in the late 1980s and was documented in detail by Sprintall and Tomczak (1992) (ST92). That study named this layer of increased stratification the barrier layer (hereafter, BL) and defined it as the difference in depths between the mixed layer and the isothermal layer. ST92 identified three regions of the tropical oceans as being favorable for BL formation: the Bay of Bengal, the South Western Pacific, and the Eastern Caribbean. The source of freshwater in the first two regions comes from heavy precipitation over the ocean during the rainy season, and the latter by the extension of the Amazon-Orinoco freshwater river plume, which can penetrate as far as north of Puerto Rico and eastward into the main development region for TCs (Foltz and McPhaden, 2009; Rudzin et al., 2017; Rudzin et al., 2018).

The location of the BL in the Caribbean has been given special attention over the past couple decades. Multiple studies note that high sea surface temperatures (SSTs) coincide with the Amazon-Orinoco river plume, and that subsurface temperature maxima are common features beneath the plume. (Sprintall and Tomczak, 1992; Pailler et al., 1999; Mignot et al., 2012). It is not uncommon for a TC to pass over the plume during the summer months, when the river freshwater extent is at a maximum. Balaguru et al. (2012) observed that when Hurricane Omar in 2008 passed over a thick BL region near the Lesser Antilles, SST cooling abruptly ceased and even warmed slightly, during which time Omar intensified from a category 1 to a category 4 storm. This was followed up with a statistical analysis of TCs around the globe from 1998-2007, and it was found that when interaction with a BL occurred, the intensification rate increased by roughly 1.5 times, SST cooling was reduced by 36%, and the mean enthalpy flux out of the ocean increased by 7%, compared to the rate over the open ocean. Results from a high resolution coupled climate model showed similar results. Reul et al. (2014) was similarly motivated by the passage of Hurricane Igor in 2010 over the Amazon river plume, during which time SST cooling decreased dramatically. Their calculations showed that the impact of the BL on cooling is directly related to the translation speed of the storm as well as its intensity.

Here, a fully coupled 3D numerical model is used to simulate the response of the TC intensity to ocean regimes of differing BL thicknesses in an idealized framework. As the response of the ocean is dependent on the residence time of the passing storm, translation speed is also varied, to get a sense of how the SST field reacts to various forcing durations (Price et al., 1986; Yablonski and Ginis, 2009; Samson et al., 2009). Section 2 describes the model used and the experimental set-up, Section 3 discusses the results from the simulations, and Section 4 summarizes the findings.

2 Methods

2.1 Model Description

The numerical model utilized in all simulations was the Weather Reserach and Forecast Model (WRF) version 3.9.1.1 for the atmosphere, coupled to the 3D Price-Weller-Pinkel (PWP) ocean model, allowing for full two-way interaction. 3D PWP is based on the work of Price et al. (1986) and Price et al. (1994), and describes the evolution of the upper ocean to surface wind stresses. The potential for vertical mixing is based on the mixed layer and sub-pycnocline density stratification, thus taking into account the effects of salinity on density, making it a desirable model for this study. Included are horizontal ocean processes such as advection and upwelling, which are often neglected in numerical ocean studies with the assumption that horizontal processes are dominated by ver-

*Corresponding Author Address: James Hlywiak, University of Miami, Rosenstiel School of Marine and Atmospheric Science, Miami, FL, 33149. email: jhlywiak@rsmas.miami.edu

tical processes such as entrainment mixing at the base of the mixed layer and the surface heat flux.

Simulations were performed with 3 domains featuring doubly-periodic boundary conditions, over 6 days. Horizontal resolutions of 18, 6, and 2 km were chosen, covering 280x160, 180x180, and 240x240 grid points, respectively. The model used 40 vertical levels evenly spaced using the WRF pressure coordinates, with the model top at 20 km. In the ocean, 30 vertical levels were used, with 6 m resolution down to 104 m and 16 m resolution below that down to 296 m. Time-steps of 10 seconds for the atmosphere and 1 minute for the ocean were chosen. The drag coefficient scheme explained in detail by Donelan et al. (2004) was used, with a constant enthalpy exchange coefficient. The WSM5 microphysics and YSU boundary layer scheme were all enabled. Shortwave and longwave radiation as well as the cumulus parameterization were turned off.

2.2 Initialization

For each simulation, a weak initial vortex on the f-plane was embedded by the point-downscaling method of Nolan (2011) in easterly mean flow with different speeds and 2.5 m/s of westerly shear, over a horizontally homogeneous ocean featuring SSTs of 28°C. The vortex radius of maximum winds (RMW) and maximum azimuthal winds were 90 km and 20 m/s, respectively, and the Dunion (2011) moist sounding was used for the atmospheric profile. f was set to the equivalent of 12°N, coincident with observations of the Amazon-Orinoco freshwater river plume.

To test the influence of the barrier layer, idealized upper ocean salinity profiles were created, modelled after typical values observed in the Amazon freshwater plume (Figure 1, top). Each domain was initialized with the same profile across the entire grid. BL0 features a constant salinity profile of 36.5 psu with depth, while BL12 and BL24 contain equivalent linear salinity gradients of thicknesses 12 and 24 m below the mixed layer, respectively. The same temperature profile was used for all 3 salinity profiles, and was based on in-situ dropsonde data taken near the plume region. The initial isothermal depth was 50 m, and the initial mixed layer depths were 50, 38, and 24 m for the BL0, BL12, and BL24 cases. The barrier layer for each case was defined as the difference between the isothermal and mixed layer depths. The isothermal depth was determined as the depth at which the temperature departs from the 10 m temperature by 0.2°C. The mixed layer depth was defined as the depth at which the potential density increases by the same value that it would for a decrease in temperature of 0.2°C, assuming constant salinity.

TC translation speed was varied by changing the initial mean easterly flow, which were also horizontally homogeneous across each domain. Following Lloyd and Vecchi (2011) and Reul et al. (2014), translation speed was non-dimensionalized by $C = U_h/fL$, where U_h is the storm translation speed in m/s, f is the Coriolis parameter at 12°N, and L is a length scale defined here as 100 km. The ocean response to a passing TC tends to be strongest for $C \leqslant 1$ (Lloyd and Vecchi, 2011). Here, 3 different values of C are used: 0.5 (slow), 1 (medium), and 1.5 (fast), as in Figure 1, bottom. Slight variations in C occur over the course of the lifetime of each storm, however changes are assumed to be small enough that the overall results are not impacted significantly.

Overall, for 3 different atmospheric and ocean profiles, 9 unique cases were tested. 3 ensemble members were created for each case by introducing random noise to the initial vortex wind field. As a result, 27 total simulations were performed.

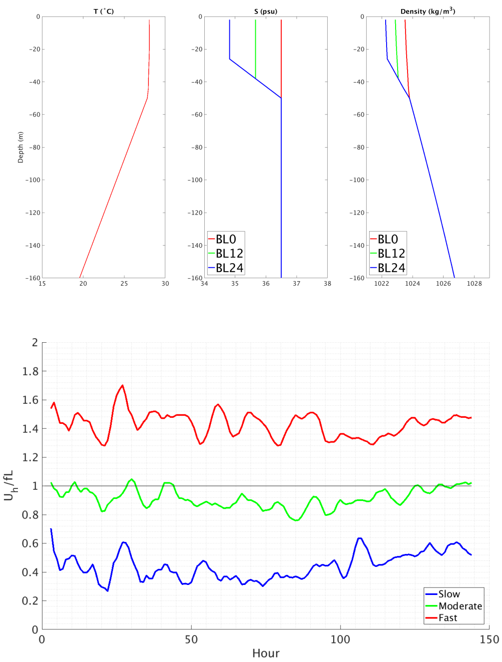

Figure 1: Top: Initial temperature (left), salinity (middle), and density (right) profiles highlighting the difference between the three initial ocean profiles. Bottom: Sample storm translation speeds for the slow (blue), medium (green), and fast (red) cases.

3 Results

3.1 BL Influence on TC Intensity

Figure 2 shows that both the translation speed and presence of the barrier layer had noticeable impacts on the overall intensities of the simulated TCs. When only considering storm motion, intensity decreased for decreasing translation speed. In fact, each value of C resulted in a different intensity trend after $t = 70$ h. For $C = 0.5$, slight

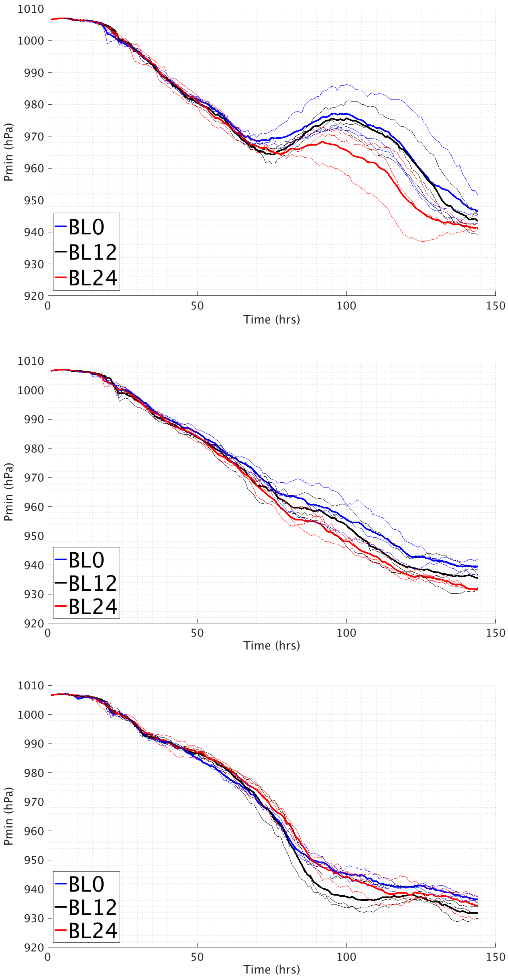

Figure 2: Storm intensity defined by minimum pressure (hPa) vs time for $C = 0.5$ (top), 1 (middle), and 1.5 (bottom) translation speed cases. Thin blue, black, and red plots indicate ensemble members for the BL0, BL12, and BL24 ocean profiles, respectively. Thick lines indicate ensemble means for each BL thickness.

weakening was observed until $t = 95$ h, at which time strengthening resumed. Re-intensification coincided with a slight deflection of the storm to the northwest, observed in all simulations. Therefore, re-intensification can most likely be attributed to the fact that as the storm motion changed direction, it encountered an unperturbed ocean regime, unaffected by the significant SST cooling at the previous time steps. For $C = 1$, intensification occurred at an essentially linear rate throughout the duration of each simulation. When $C = 1.5$, each simulation underwent rapid intensification from $t = 70$-85 h.

As storm translation speed decreases, variations in ensemble members and differences in the mean minimum pressure plots between the BL cases grew. For $C = 0.5$, the mean plots for BL0 and BL12 show similar values, but the mean BL24 values remained 10 hPa stronger than the other two. The largest range in values between BL0 and BL24 ensemble members was 40 hPa, highlighting the large ensemble member variability associated with the slow storm cases. The ensemble mean pressure plots for $C = 1$ show that the BL24 storms were on average about 10 hPa stronger than BL0 and about 5 hPa stronger than BL12. Differences between the ensemble mean pressure plots were smaller, but still significant. Differences in mean minimum pressure for $C = 1.5$ were greatly reduced, and the thickness of the BL appears to have had little effect on intensity, except for a brief period between $t = 85 - 115$ h, when the BL24 case reached a lower minimum pressure than the other two cases.

The divergence in the plots after $t = 70$ h is significant because by this time, all storms had reached at least category 3 hurricane designation (49.6 m/s, velocity maximum plots not shown). This implies that wind speeds less than that are not strong enough to initiate entrainment mixing at the depth of the mixed layer for BL24. It wasn't until $t = 70$ h that each storm reached an intensity at which oceanic mixing becomes influenced by the barrier layer. Therefore, barrier layer influence must not only be a function of translation speed and BL thickness, but also storm intensity.

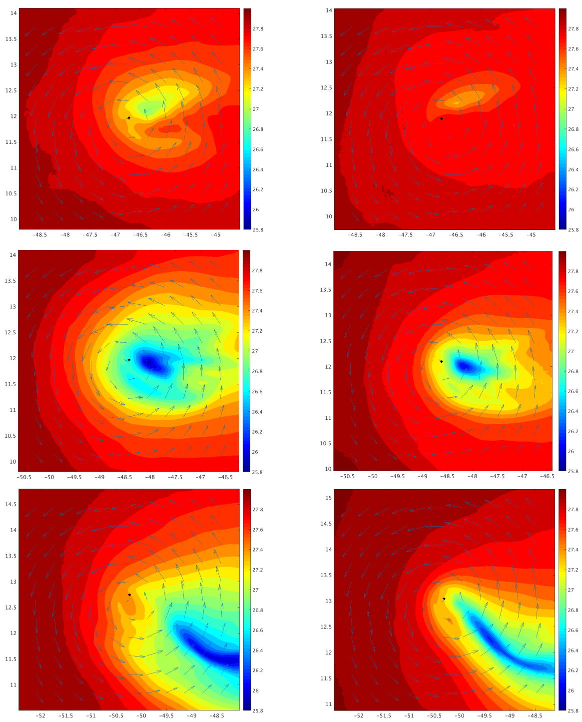

Figure 3: SST cooling for 2 ensemble members from the slow storm case. The black plus indicates the storm center, and vectors indicate surface winds. Left (right): weakest BL0 (strongest BL24) simulations from Figure 2. Top: $t = 50$ h; middle: $t = 80$ h; bottom: $t = 110$ h.

3.2 Ocean Response

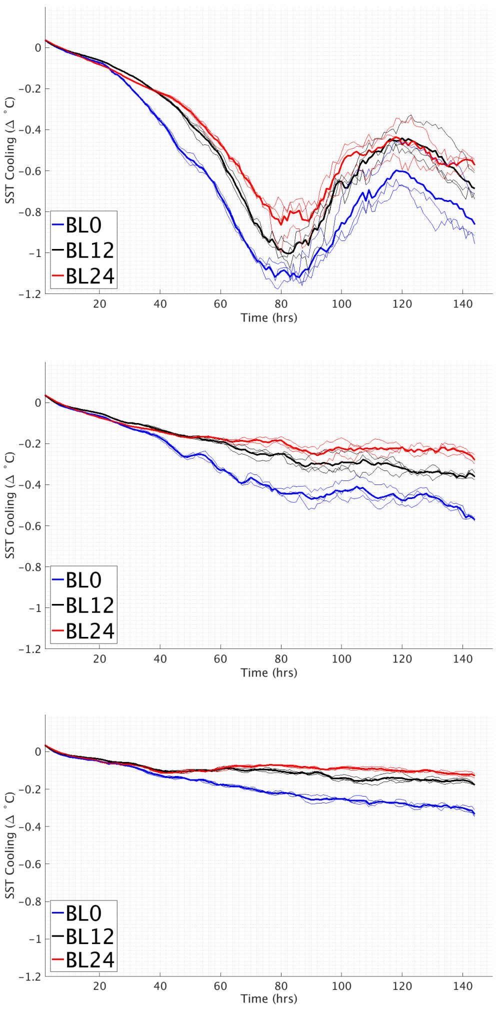

Figure 4: Mean SST change within 100 km of the storm center (°C/km2) vs time for the slow (top), medium (middle), and fast (bottom) translation speed cases. As in Figure 2, the light blue, black, and red plots indicate ensemble members for the BL0, BL12, and BL24 ocean profiles, respectively. Thick lines indicate ensemble means.

The impact of the BL thickness on the spatial and temporal variation of SST helps to explain the large differences in ensemble mean intensity. Figure 3 shows contour plots of SST for the weakest BL0 (left) and the strongest BL24 (right) ensemble members for $C = 0.5$ at $t = 50$, 80, and 110 h, when both storms were category 1 hurricanes, near the beginning of the spread in intensities, and when the ensemble intensity spread was near a maximum, respectively. Both members were integrated forward in time from vortices featuring the same initial random wind field noise, allowing for a more direct comparison. The magnitude of SST cooling in the BL0 case was much greater beneath and in the vicinity of the storm core. A rightward cooling bias is seen in both cases, but again is much more pronounced when the barrier layer is absent.

Figure 4 shows the azimuthally averaged SST cooling, averaged within 100 km of the TC center, as a function of time for each case. The overall core-cooling magnitude and ensemble variation both increase with decreasing translation speed. A clear relationship between barrier layer thickness and cooling within the TC core also arises beginning within the first 40 h in each case, providing evidence that increased thickness suppressed SST cooling. The decrease in cooling magnitude for the $C = 0.5$ cases around $t = 85$ h was due to the storm deflection to the northwest, as discussed in Section 3.1.

Finally, Figure 5 shows cross sections of the subsurface ocean beneath the same ensemble members as in Figure 3. The cross section was taken along a constant latitude through the TC center (shown by the black 'X') at $t = 80$ h. When the BL was present, SST cooling was reduced, as well as entrainment mixing at the base of the mixed layer. A much greater ocean response is observed in the slow case, in the form of deeper mixing and greater SST cooling. Another interesting feature appears in the BL24 plots through the subsurface temperature max that can be seen 20-50 m deep ahead of the center, marked by the black ovals in Figure 5. A possible explanation for this could be that the increased stability associated with the BL is preserving high temperatures beneath the mixed layer.

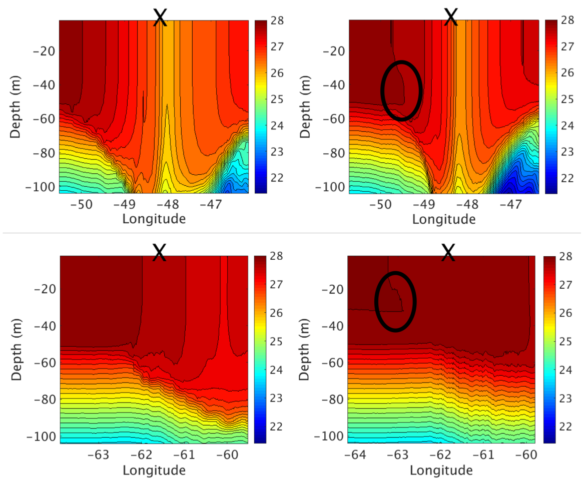

Figure 5: Subsurface ocean temperature at a constant longitude, centered on the storm center (marked by the black 'x') at $t = 80$ h. Left: BL0; right: BL24. Top: Slow case ensemble members from Figure 4; bottom: Randomly selected fast case ensemble members. The black ovals indicate the locations of sub-surface temperature maxima ahead of the storm in the BL cases.

4 Summary

In this study, a fully coupled, 3D numerical model in an idealized framework was utilized to show that the oceanic BL indirectly affects TC intensity by stabilizing the upper ocean and reducing SST cooling due to wind forcing. The degree of influence that the presence of the BL exerts on a TC was shown to be a function of BL thickness in the ocean and storm translation speed and intensity in the atmosphere. Higher variability in intensity between ensemble members and different cases exists for lower storm translation speeds and higher intensities. Future work will include a comparison of the 1D PWP ocean model to these results, to determine if 3D processes are crucial to accurately represent interactions between the ocean and a passing TC.

Acknowledgements

J. Hlywiak was supported by a University of Miami Graduate Fellowship and D. Nolan was supported by NSF PREEVENTS Track 2 Award 1663947. We would also like to thank Johna Rudzin of the University of Miami for providing temperature data used in all simulations.

References

Balaguru, K., P. Chang, R. Saravanan, R. L. Leung, Z. Xu, M. Li, and J. S. Hsieh (2012). "Ocean barrier layers' effect on tropical cyclone intensification." *PNAS* 109.39, pp. 14343–14347. URL: 10.1073/pnas.1201364109.

Donelan, MA, BK Haus, Nicolas Reul, WJ Plant, M Stiassnie, HC Graber, OB Brown, and ES Saltzman (2004). "On the limiting aerodynamic roughness of the ocean in very strong winds". *Geophysical Research Letters* 31.18.

Dunion, Jason P (2011). "Rewriting the climatology of the tropical North Atlantic and Caribbean Sea atmosphere". *Journal of Climate* 24.3, pp. 893–908.

Foltz, G.R. and M.J. McPhaden (2009). "Impact of Barrier Layer Thickness on SST in the Central Tropical North Atlantic." *J. Climate.* 22, pp. 285–299. DOI: 10.1175/2008JCLI2308.1.

Lloyd, I.D. and G.A. Vecchi (2011). "Observational Evidence for Oceanic Controls on Hurricane Intensity." *J. Climate* 24, pp. 1138–1153. URL: 10.1175/2010JCLI3763.1.

Mignot, J., A. Lazar, and M. Lacarra (2012). "On the formation of barrier layers and associated vertical temperature inversions: A focus on the northwestern tropical Atlantic." *J. Geophys. Res.* 117. URL: 10.1029/2011JC007435.

Nolan, D.S. (2011). "Evaluating Environmental Favorableness for Tropical Cyclone Development with the Method of Point-Downscaling." *J. Adv. Model. Earth Syst.* 3.M08001, p. 28. URL: 10.1029/2011MS000063.

Pailler, K, B Bourles, and Y Gouriou (1999). "The Barrier Layer in the Western Tropical Atlantic Ocean." *Geophysical Research Letters.* 26, pp. 2069–2072. URL: 10.1029/1999GL900492.

Price, J. F., R. A. Weller, and R. Pinkel (1986). "Diurnal cycling: Observations and models of the upper ocean response to diurnal heating, cooling, and wind mixing." *J. Geophys. Res.* 91, pp. 8411–8427. URL: 10.1029/JC091iC07p08411.

Price, J.F., T.B. Sanford, and G.Z. Forristall (1994). "Forced Stage Response to a Moving Hurricane." *J. Phys. Oceanogr.* 24, pp. 233–260. URL: 10.1175/1520-0485(1994)024%3C0233:FSRTAM%3E2.0.CO;2.

Reul, N., Y. Quilfen, B. Chapron, S. Fournier, V. Kudryavtsev, and R. Sabia (2014). "Multisensor observations of the Amazon-Orinoco river plume interactions with hurricanes." *J. Geophys. Res.* 119, pp. 8271–8295. URL: 10.1002/2014JC010107.

Rudzin, JE, LK Shay, B Jaimes, and JK Brewster (2017). "Upper ocean observations in eastern caribbean sea reveal barrier layer within a warm core eddy". *Journal of Geophysical Research: Oceans* 122.2, pp. 1057–1071.

Rudzin, Johna E, Lynn K Shay, and William E Johns (2018). "The influence of the barrier layer on SST response during tropical cyclone wind forcing using idealized experiments". *Journal of Physical Oceanography* 2018.

Samson, Guillaume, Hervé Giordani, Guy Caniaux, and Frank Roux (2009). "Numerical investigation of an oceanic resonant regime induced by hurricane winds". *Ocean Dynamics* 59.4, pp. 565–586. ISSN: 1616-7228. DOI: 10.1007/s10236-009-0203-8. URL: https://doi.org/10.1007/s10236-009-0203-8.

Sprintall, J. and M Tomczak (1992). "Evidence of the Barrier Layer in the Surface Layer of the Tropics." *Journal of Geophysical Research.* 27, pp. 7305–7316.

Yablonski, R.M. and I. Ginis (2009). "Limitation of One-Dimensional Ocean Models for Coupled Hurricane-Ocean Model Forecasts." *Monthly Weather Review* 137, pp. 4410–4419.